Experimental and modeling investigation of the low-temperature oxidation of dimethylether

Anne Rodriguez[1], Ophélie Frottier[1], Olivier Herbinet[1], René Fournet[1], Roda Bounaceur[1], Christa Fittschen[2], Frédérique Battin-Leclerc[1]

[1]Laboratoire Réactions et Génie des Procédés, CNRS, Université de Lorraine, BP 20451, 1 rue Grandville, 54000 Nancy, France

[2]PhysicoChimie des Processus de Combustion et de l'Atmosphère, CNRS, Université Lille Nord de France, 59650 Villeneuve d'Ascq, France

Supplemental Data

Table of content

1) Comparison of JSR data obtained in this study with data computed using literature models - Symbols represent literature experimental data and lines the simulations using the present model

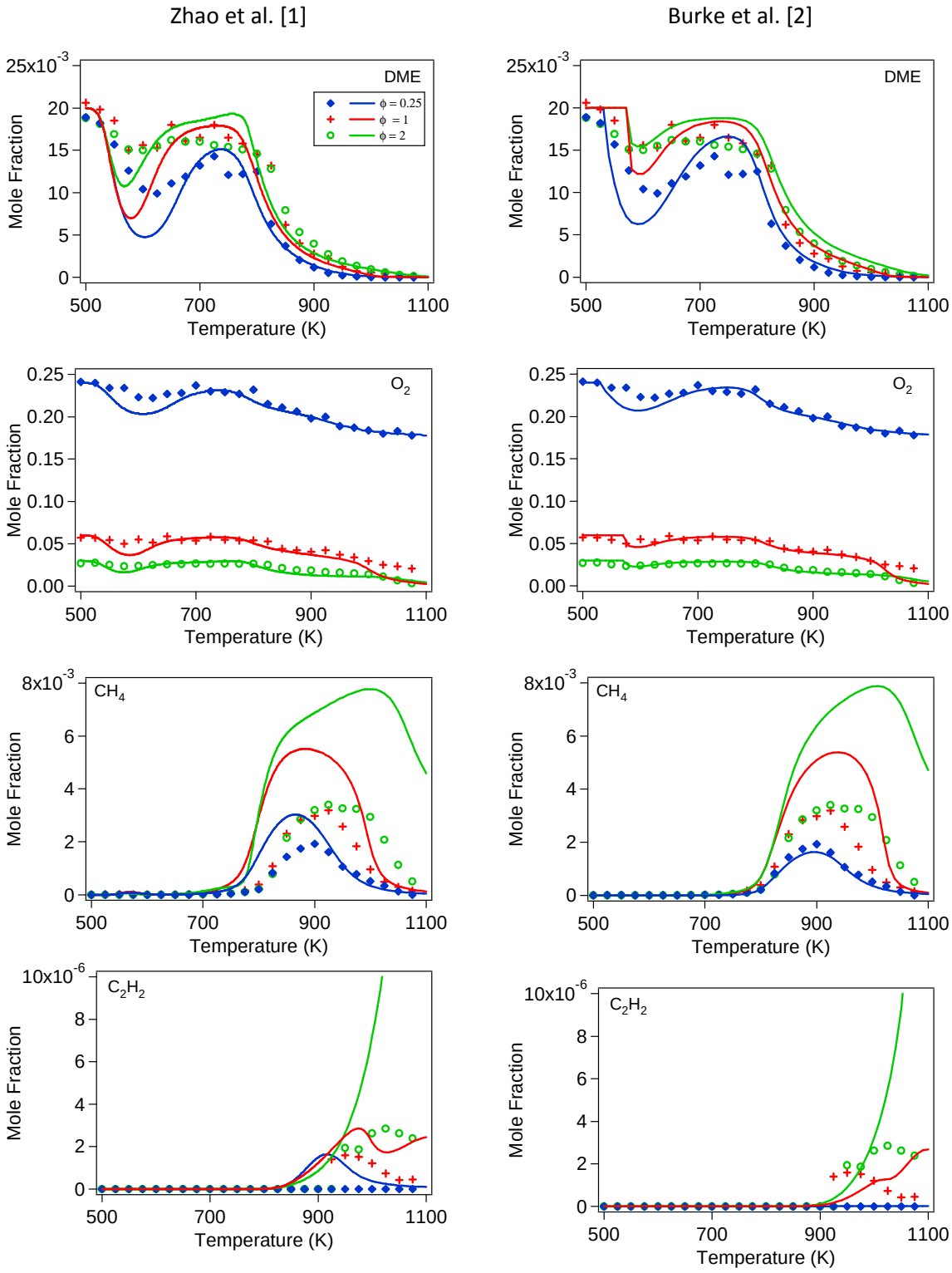

Figure S1: Comparison between our experimental data and predictions using models of the literature: Zhao et al. [1] on the left, Burke et al. [2] on the right.

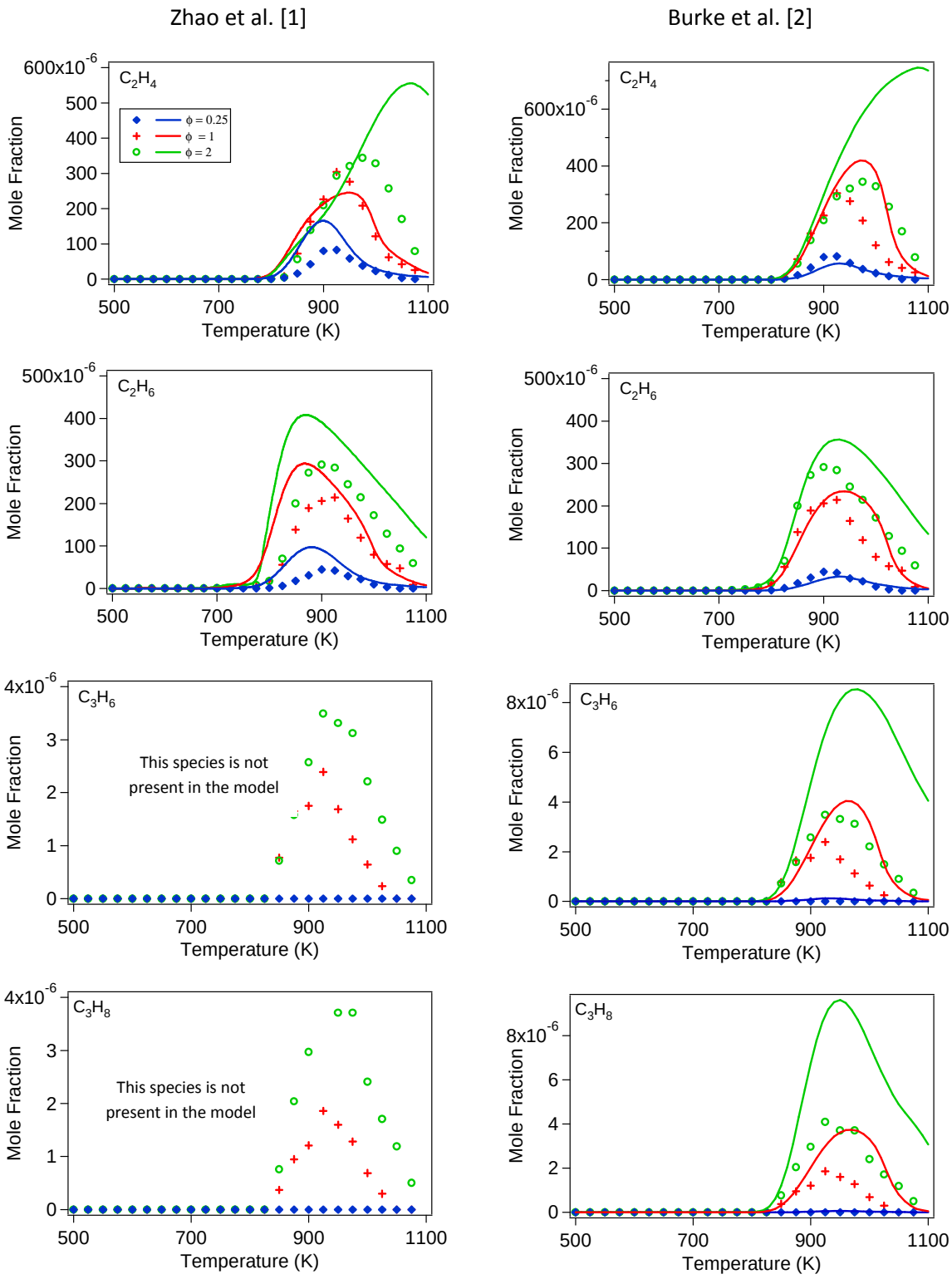

Figure S2: Comparison between our experimental data and predictions using models of the literature: Zhao et al. [1] on the left, Burke et al. [2] on the right.

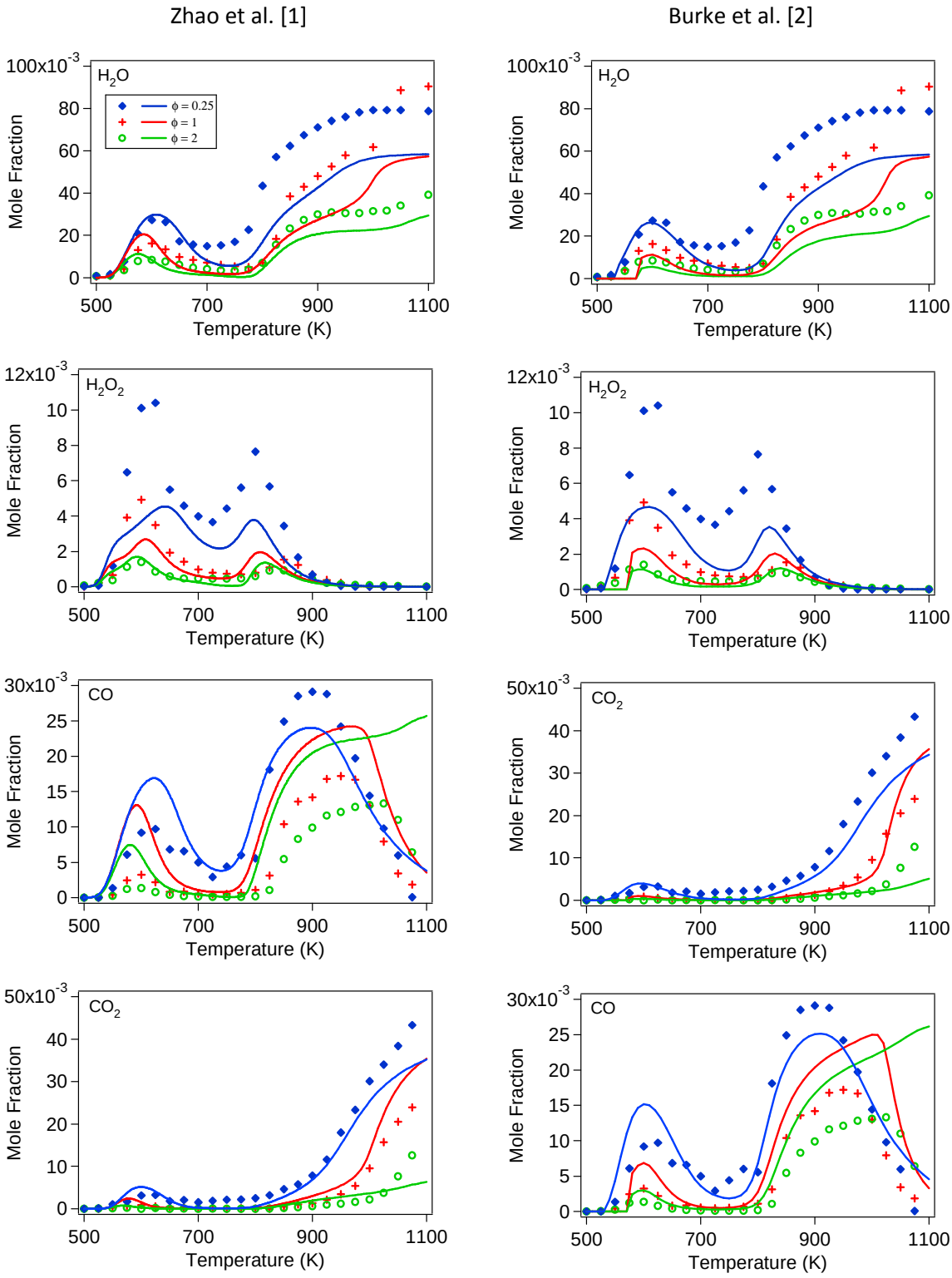

Figure S3: Comparison between our experimental data and predictions using models of the literature: Zhao et al. [1] on the left, Burke et al. [2] on the right.

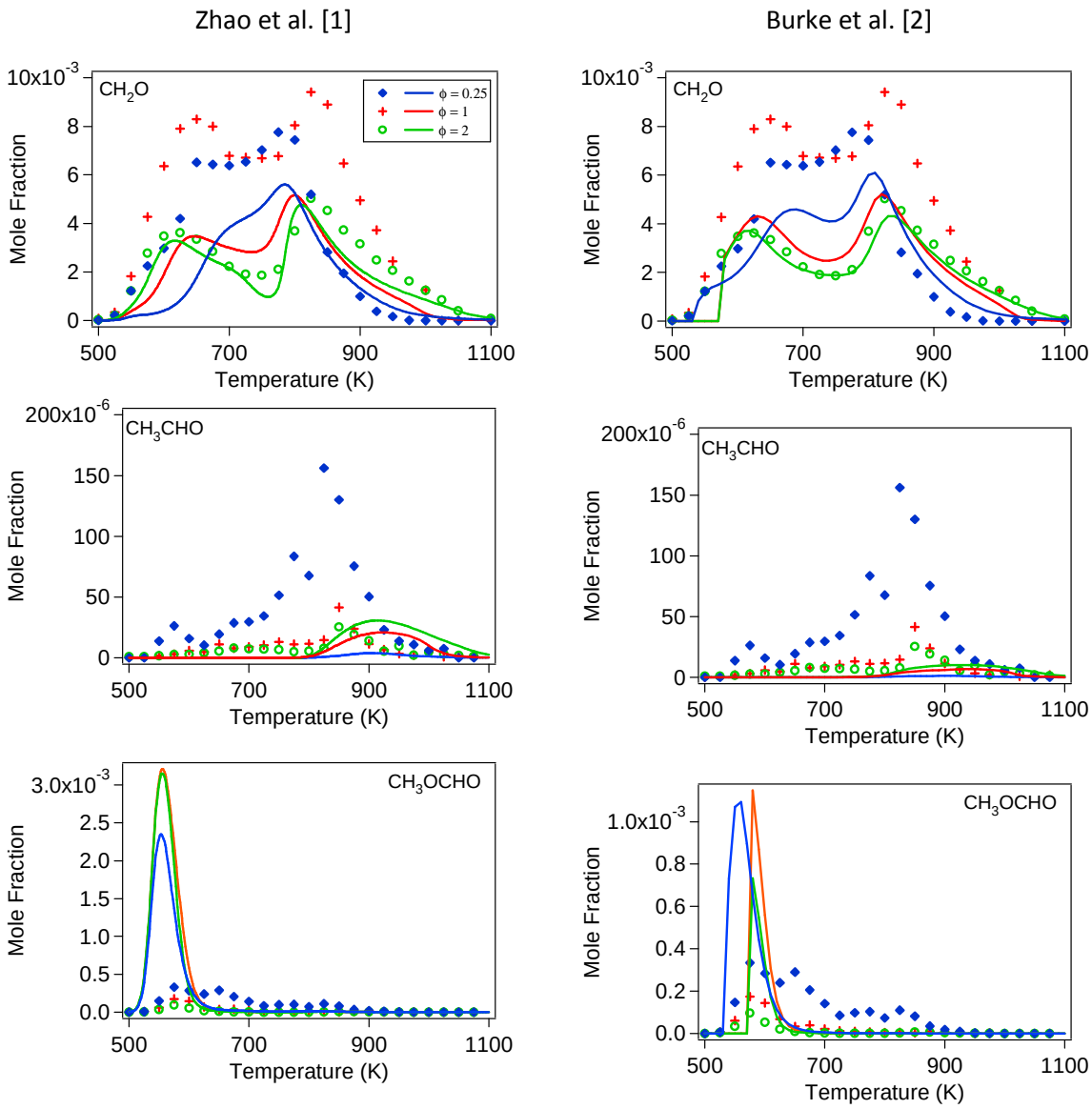

Figure S4: Comparison between our experimental data and models predictions using models of the literature: Zhao et al. [1] on the left, Burke et al. [2] on the right.

2) Reactions included in the mechanism for the consumption methyl-formate (not shown in the main text)

Table S1: Reactions included in the methyl-formate oxidation sub-mechanism. Kinetic parameters of the form $k = A \times T^n \times exp(-E_a/RT)$. Units: cm^3, mol, s, cal.

Reactions	A	n	E_a	reference
Unimolecular Initiation				
$CH_3OCHO = CH_3O^\bullet + {}^\bullet CHO$	0.85×10^{42}	-7.95	91.80×10^3	[a]
$CH_3^\bullet + {}^\bullet OCHO = CH_3OCHO$	3.00×10^{13}	0	0	[a]
$H^\bullet + {}^\bullet CH_2OCHO = CH_3OCHO$	1.00×10^{14}	0	0	[3]
$H^\bullet + CH_3OC^\bullet O = CH_3OCHO$	1.00×10^{14}	0	0	[3]
Bimolecular Initiation				
$CH_3OCHO + O_2 = {}^\bullet CH_2OCHO + {}^\bullet OH$	2.05×10^{13}	0	44.91×10^3	[a]
$CH_3OCHO + O_2 = CH_3OC^\bullet O + {}^\bullet OH$	1.00×10^{13}	0	49.70×10^3	[4,5]
H-atom Abstraction				
$CH_3OCHO + H^\bullet = CH_3OC^\bullet O + H_2$	2.72×10^7	1.94	7880	[6]
$CH_3OCHO + H^\bullet = {}^\bullet CH_2OCHO + H_2$	1.42×10^7	2.05	8884	[6]
$CH_3OCHO + {}^\bullet O^\bullet = CH_3OC^\bullet O + {}^\bullet OH$	2.35×10^5	2.50	2230	[4,5]
$CH_3OCHO + {}^\bullet O^\bullet = {}^\bullet CH_2OCHO + {}^\bullet OH$	8.99×10^{12}	0	5.37×10^3	[7]
$CH_3OCHO + {}^\bullet OH = CH_3OC^\bullet O + H_2O$	1.61×10^6	1.87	26.3	[6]
$CH_3OCHO + {}^\bullet OH = {}^\bullet CH_2OCHO + H_2O$	2.13×10^6	2.00	1458	[6]
$CH_3OCHO + HO_2^\bullet = CH_3OC^\bullet O + H_2O_2$	1.22×10^{12}	0	17.0×10^3	[4,5]
$CH_3OCHO + HO_2^\bullet = {}^\bullet CH_2OCHO + H_2O_2$	3.00×10^{12}	0	14.0×10^3	[3]
$CH_3OCHO + CH_3^\bullet = CH_3OC^\bullet O + CH_4$	65.64	3.32	10.0×10^3	[6]
$CH_3OCHO + CH_3^\bullet = {}^\bullet CH_2OCHO + CH_4$	13.91	3.35	11.5×10^3	[6]
$CH_3OCHO + {}^\bullet CHO = CH_3OC^\bullet O + HCHO$	1.80×10^{11}	0	12.9×10^3	[8]
$CH_3OCHO + {}^\bullet CHO = {}^\bullet CH_2OCHO + HCHO$	1.02×10^5	2.50	13.5×10^3	[3]
$CH_3OCHO + CH_3O^\bullet = CH_3OC^\bullet O + CH_3OH$	5.48×10^{11}	0	5.0×10^3	[4,5]
$CH_3OCHO + CH_3O^\bullet = {}^\bullet CH_2OCHO + CH_3OH$	6.90×10^{10}	0	2.9×10^3	[3]
Reactions of $^\bullet CH_2OCHO$				
$^\bullet CH_2OCHO = HCHO + {}^\bullet CHO$	4.45×10^{14}	-0.22	27.2×10^3	[b]
$^\bullet CH_2OCHO + O_2 = {}^\bullet O_2CH_2OCHO$	3.39×10^{11}	0	-1699	[c]
Isomerization of $^\bullet O_2CH_2OCHO$				
$^\bullet O_2CH_2OCHO = HO_2CH_2OC^\bullet O$	6.00×10^{10}	0	16.5×10^3	[3]
Reactions of $HO_2CH_2OC^\bullet O$				
$HO_2CH_2OC^\bullet O => CO_2 + HCHO + {}^\bullet OH$	1.50×10^{13}	0	20.5×10^3	[3]
$HO_2CH_2OC^\bullet O = CO + HO_2CH_2O^\bullet$	2.00×10^{13}	0	17.15×10^3	[3]
$HO_2CH_2OC^\bullet O = C2H2O3\#4 + {}^\bullet OH$	2.50×10^{10}	0	15.25×10^3	[3]
$HO_2CH_2O^\bullet = HCHO + HO_2^\bullet$	1.28×10^{12}	0	13.5×10^3	[9]

Table S1 (continued)

Reactions of $^{\bullet}CH_2OCHO$				
$CH_3OC^{\bullet}O + O2 = CH_3OC(OO^{\bullet})O$	3.39×10^{11}	0	-1699	[c]
Isomerization of $CH_3OC(OO^{\bullet})O$				
$CH_3OC(OO^{\bullet})O = {}^{\bullet}CH_2OC(OOH)O$	3.70	3.347	15212	[d]
Decomposition of $^{\bullet}CH_2OC(OOH)O$				
${}^{\bullet}CH_2OC(OOH)O \Rightarrow HCHO + CO_2 + {}^{\bullet}OH$	1.50×10^{13}	0	20.5×10^{3}	[e]

[a] rate constant taken equal as for DME with an A factor divided by a factor of 2
[b] rate constant taken equal as $CH_3OCH_2^{\bullet} = HCHO + CH_3^{\bullet}$
[c] rate constant taken equal as $CH_3OCH_2^{\bullet} + O_2 = CH_3OCH_2O_2^{\bullet}$
[d] rate constant taken equal as $CH_3OCH_2O_2^{\bullet} = {}^{\bullet}CH_2OCH_2O_2H$
[e] rate constant taken equal as ${}^{\bullet}CH_2OCH_2O_2H \Rightarrow 2\ HCHO + {}^{\bullet}OH$

3) Key reactions during the simulations of the oxidation of DME for fuel consumption

Table S2: Key reactions during the simulations of the JSR DME oxidation under conditions of figures 2 to 4. Reactions are numbered in the second column as in the mechanism (see Supporting Information). The separation line in the table indicates reactions of reaction base and DME sub-mechanisms, respectively.

	n°reaction	Reaction
1	16	CH3 + CH3 → C2H5 + H
2	18	H + CH3(+M) → CH4(+M)
3	23	CH4 + CH2 → CH3 + CH3
4	79	O + C2H6 → C2H5 + OH
5	98	OH + C2H3V → C2H2T + H2O
6	120	CHO + C2H3V → C2H4 + CO
7	134	HCHO + OH → CHO + H2O
8	171	CH2OH + CHO → HCHO + HCHO
9	232	C2H4OE#3 + H → H2O + C2H3V
10	250	C2H4OH → H + CH3CHO
11	277	O2 + H → OH + O
12	290	O2 + CH3(+M) → CH3OO(+M)
13	305	O2 + C2H5 → CH3CHO + OH
14	327	OOH + CH3 → CH3O + OH
15	340	OOH + HCHO → CHO + H2O2
16	347	OOH + OOH → H2O2 + O2
17	348	OOH + OOH → H2O2 + O2
18	377	CH3OO + HCHO → CH3OOH + CHO
19	416	C2H5OO + CH3OOH → C2H5OOH + CH3OO
20	473	C3H8 + CHO → Ic3h7 + HCHO
21	488	nC3H7 + O2 → C3H6 + OOH
22	515	DME + O2 → CH3OCH2 + OOH
23	516	DME + OH → H2O + CH3OCH2
24	517	DME + H → H2 + CH3OCH2
25	520	DME + CHO → HCHO + CH3OCH2
26	525	CH3OCH2OO → CH2OCH2OOH
27	527	CH2OCH2OOH → HCHO + HCHO + OH
28	529	CH2OCH2OOH → CH3OCHO + OH
29	530	CH2OCH2OOH + O2 → OOCH2OCH2OOH
30	533	CH3OCH2OO + CH3OCH2OO → CH3OCH2O + CH3OCH2O + O2
31	537	HOOCH2OCHO → OH + OCH2OCHO
32	540	OCHO → CO2 + H
33	544	C2H4O2#4 + OOH → H2O2 + HCHO + CHO
34	553	CH3OCHO + OH → CH2OCHO + H2O
35	574	CH3OCO + O2 → CH3OCOOO

4) Data flux analyses not shown in the main text

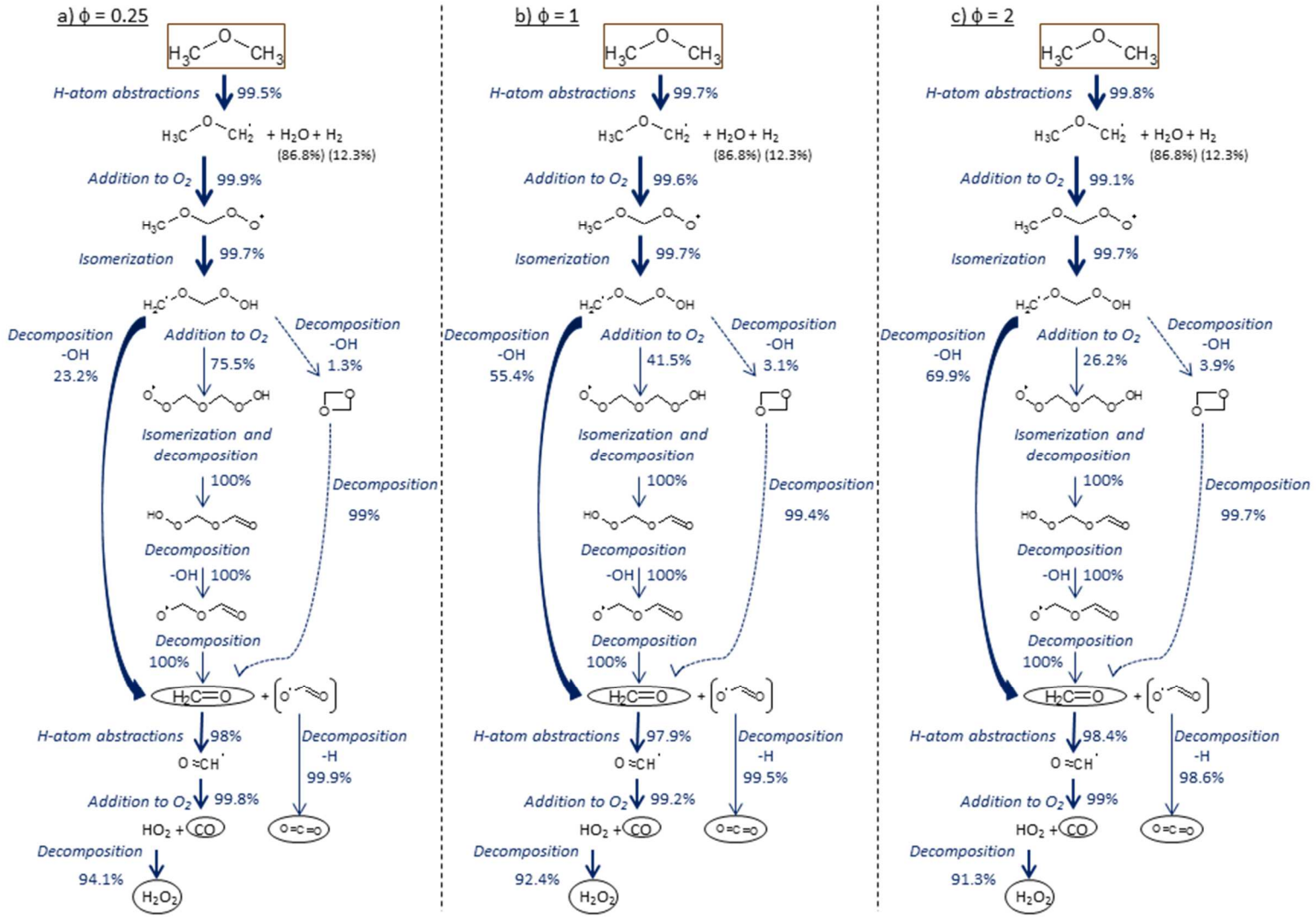

Figure S5: Comparison of data flux analysis at the three studied equivalence ratios. (a) φ = 0.25, (b) φ = 1 and (c) φ = 2 (the temperature is 625K).

5) Comparisons of simulations using the present model with literature data not shown in the main text - Symbols represent literature experimental data and lines the simulations using the present model.

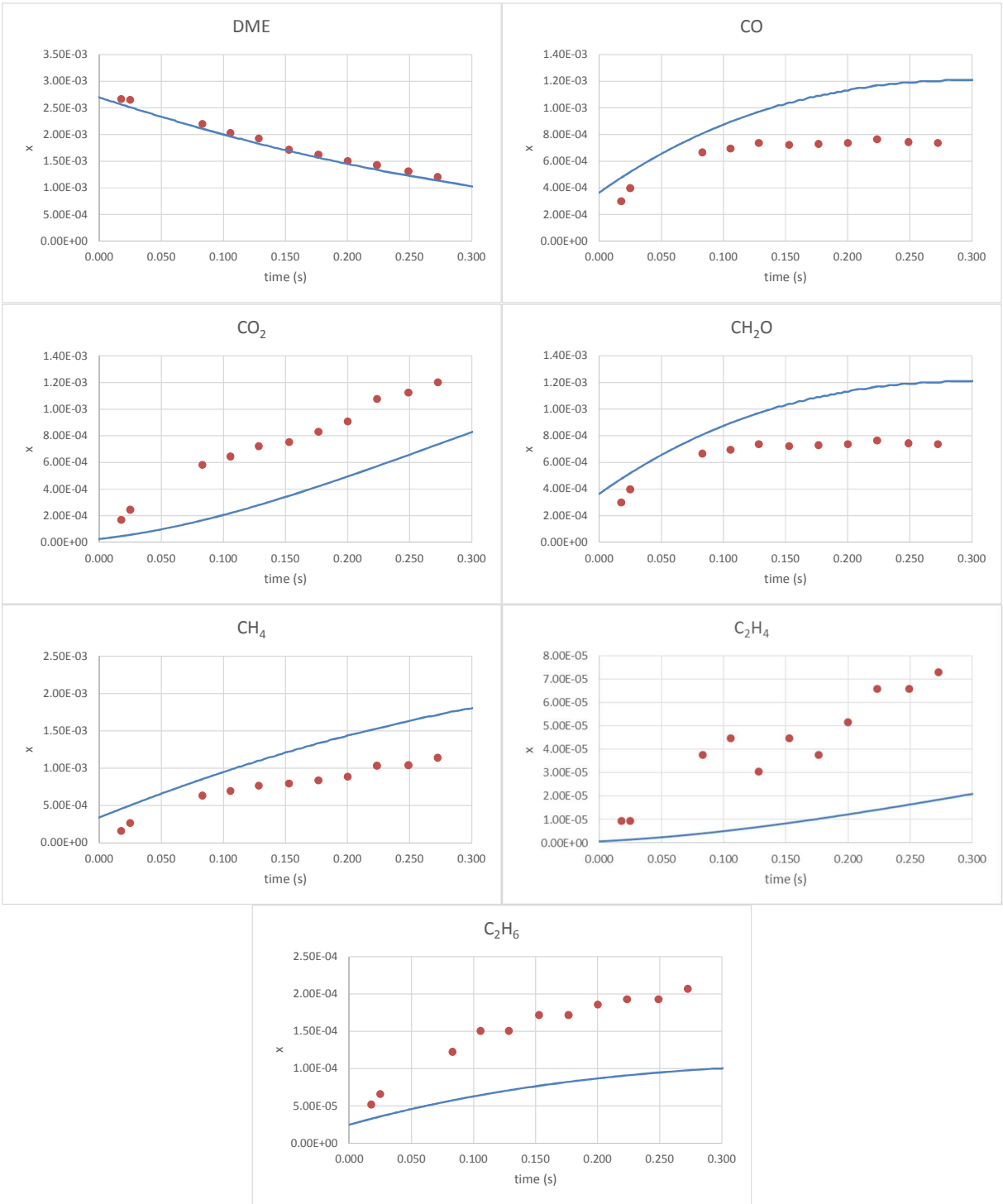

Figure S6: Comparison with flow tube pyrolysis data from Fischer et al. [4] (P = 2.5 bar, x_{fuel} = 0.00309, dilution in N_2). Simulations were shifted by 50 ms as recommended by Fischer et al.

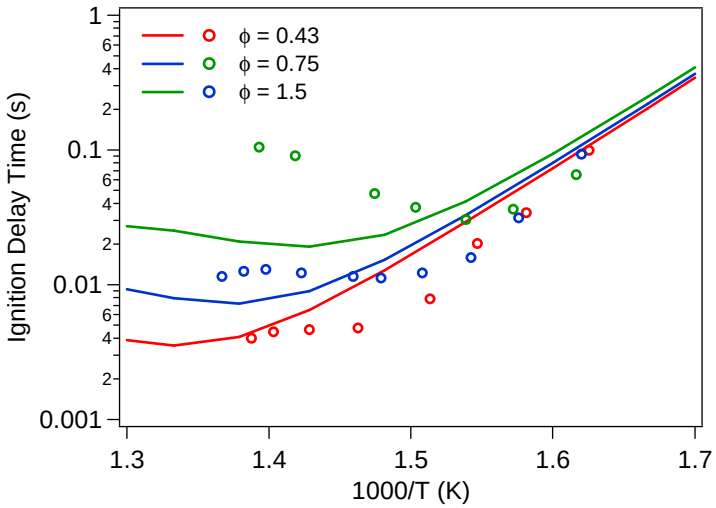

Figure S7: Comparison with rapid compression machine data from Mittal et al. [10] (P = 10 bar, x_{fuel} = 2.86×10^{-2}, dilution in N_2).

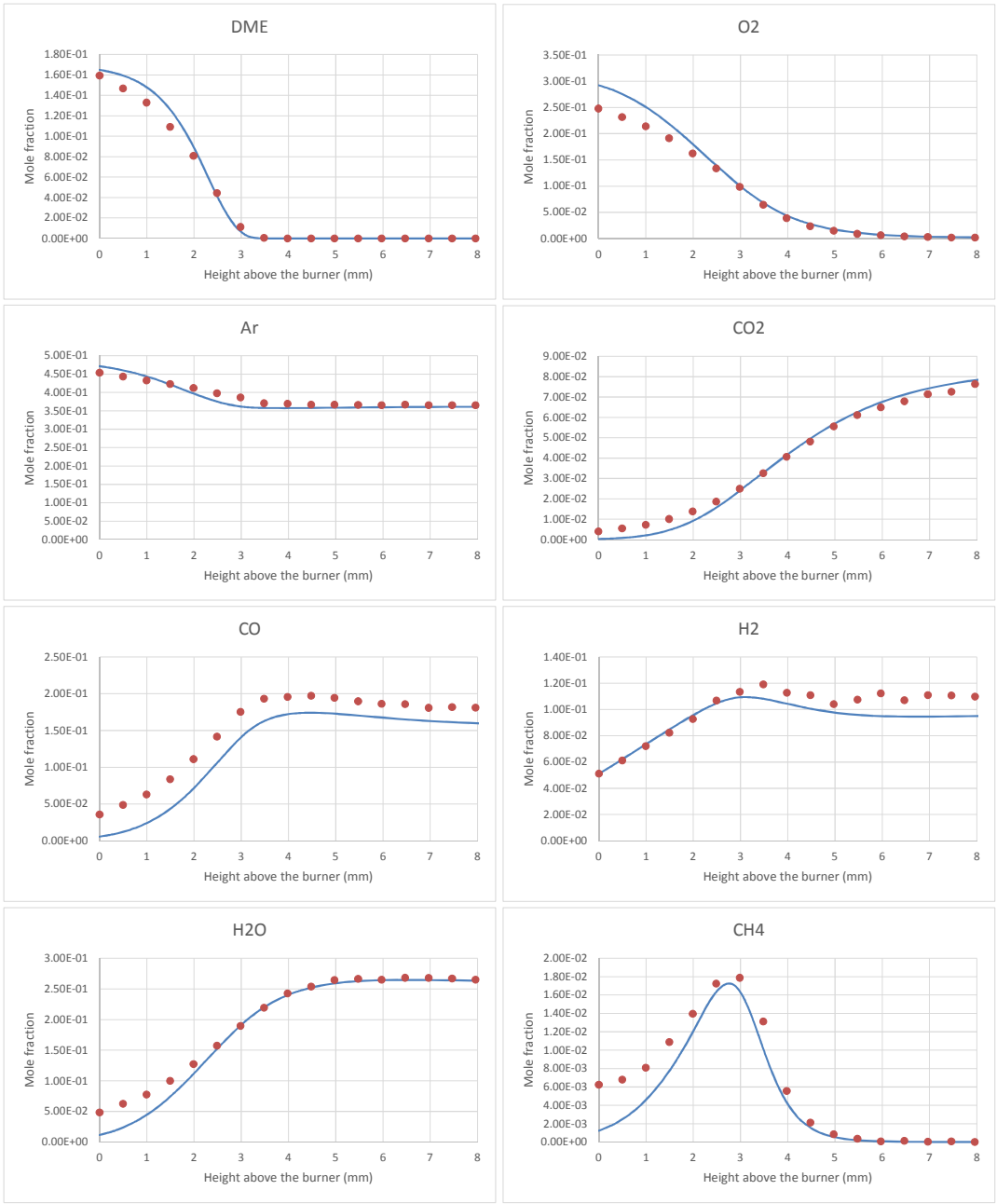

Figure S8: Comparison with flame structure data from Liu et al. [11] (P = 50 mbar, $\varphi = 2.6$, x_{fuel} = 0.1758, x_{oxygen} = 0.3242, dilution in Ar). Simulations were made using the temperature profile given by the authors.

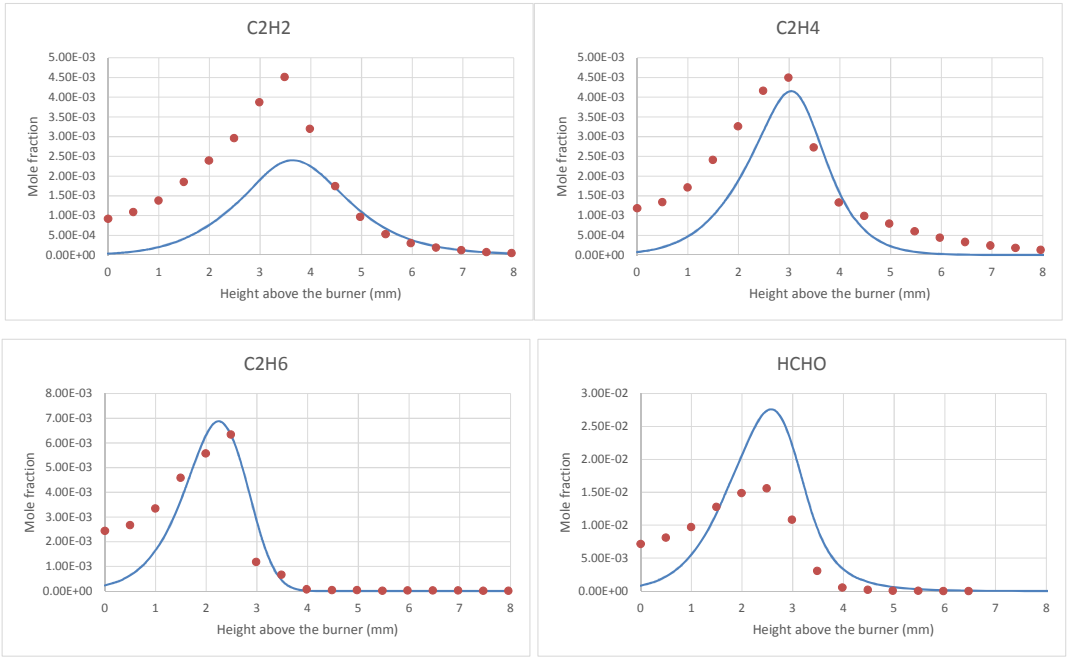

Figure S9: Comparison with flame structure data from Liu et al. [11] (P = 50 mbar, $\varphi = 2.6$, x_{fuel} = 0.1758, x_{oxygen} = 0.3242, dilution in Ar). Simulations were made using the temperature profile given by the authors.

References

[1] Z. Zhao, M. Chaos, A. Kazakov, F.L. Dryer, Int. J. Chem. Kinet. 40 (2008) 1.

[2] U. Burke, K.P. Somers, P. O'Toole, C.M. Zinner, N. Marquet, G. Bourque, E.L. Petersen, W.K. Metcalfe, Z. Serinyel, H.J. Curran, Combust. Flame (n.d.).

[3] F. Buda, R. Bounaceur, V. Warth, P.A. Glaude, R. Fournet, F. Battin-Leclerc, Combust. Flame 142 (2005) 170.

[4] S.L. Fischer, F.L. Dryer, H.J. Curran, Int. J. Chem. Kinet. 32 (2000) 713.

[5] H.J. Curran, S.L. Fischer, F.L. Dryer, Int. J. Chem. Kinet. 32 (2000) 741.

[6] D.A. Good, J.S. Francisco, J. Phys. Chem. A 106 (2002) 1733.

[7] J.T. Herron, J. Phys. Chem. Ref. Data 17 (1988) 967.

[8] W. Tsang, R.F. Hampson, J. Phys. Chem. Ref. Data 15 (1986) 1087.

[9] F. Herrmann, B. Jochim, P. Oßwald, L. Cai, H. Pitsch, K. Kohse-Höinghaus, Combust. Flame 161 (2014) 384.

[10] G. Mittal, M. Chaos, C.-J. Sung, F.L. Dryer, Fuel Process. Technol. 89 (2008) 1244.

[11] D. Liu, J. Santner, C. Togbé, D. Felsmann, J. Koppmann, A. Lackner, X. Yang, X. Shen, Y. Ju, K. Kohse-Höinghaus, Combust. Flame 160 (2013) 2654.